Supplement of Atmos. Chem. Phys., 23, 1941–1961, 2023
https://doi.org/10.5194/acp-23-1941-2023-supplement

Atmospheric Chemistry and Physics
Open Access

Supplement of

Observations of microphysical properties and radiative effects of a contrail cirrus outbreak over the North Atlantic

Ziming Wang et al.

Correspondence to: Ziming Wang (ziming.wang@dlr.de) and Luca Bugliaro (luca.bugliaro@dlr.de)

S1 Air traffic dataset

For flights outside the surveillance domain of EUROCONTROL, data from EUROCONTROL's Model 3 (M3) data (Wandelt and Sun, 2015) are used, which consist of track information from departure to destination also outside Europe. The M3 data are flight plan data partly corrected by radar data and were downloaded from the data repository of EUROCONTROL. The M3 files are provided directly from the network manager archives. For flights in the Shanwick control zone of the North Atlantic flight corridor, track information was provided by North Atlantic Tracks (NATS). These were used to either replace or augment M3 data in that zone.

S2 RHi from the WALES lidar

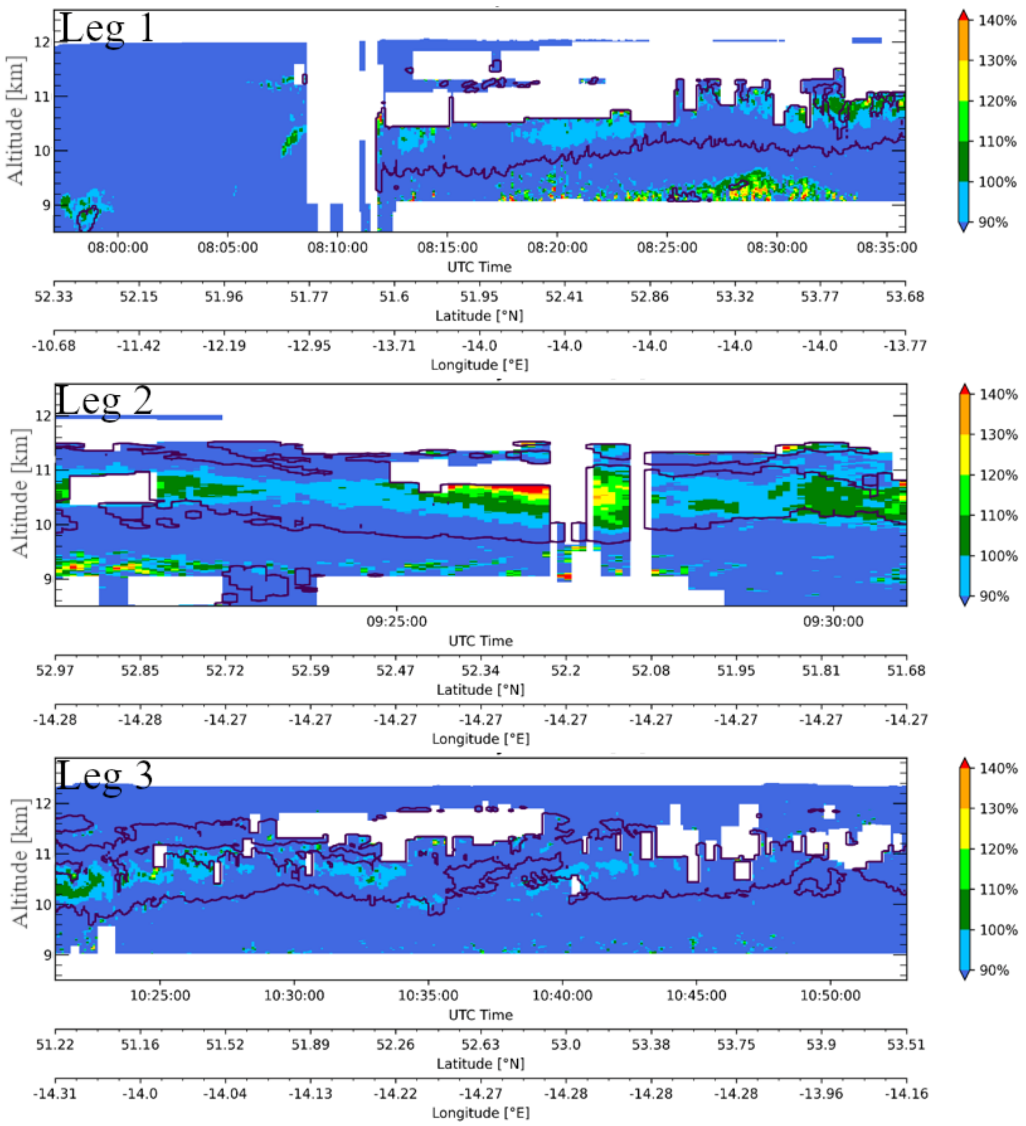

Figure S1: The three panels show the RHi from Fig. 3 in more detail. The black contour represents the cloud edge. White areas are due to lack of measurements in these regions, because of detector saturation.

S3 Identification of contrails, contrail cirrus and natural cirrus

The threshold values for ΔNO (0.02 ppbv and 0.14 ppbv) have been determined from the ΔNO distribution (Fig. S2). ΔNO distribution decreases from 0.0 to 0.48 ppbv, with the largest bins being the first and the second one (0<=ΔNO <0.02 ppbv). Thus, we consider NO to be close to the background value when ΔNO <=0.02 ppbv and to contain additional NO when ΔNO >0.02 ppbv. The NO occurrences sink by two order of magnitude (from 10^3 to 10^1) until ΔNO equals 0.25-0.30 ppbv. After these values, a tail of relatively seldom high ΔNO values (occurrences~10^1) is observed. In order to distinguish old emissions from younger ones, we select the threshold of ΔNO =0.14 ppbv, in the middle of the range mentioned above. Thus, ΔNO between 0.02 and 0.14 ppbv are assumed to capture only older emissions, leaving high NO peaks as well as moderate ones in the range ΔNO >0.14 ppbv (representing the highest 5% ΔNO). For the determination of N thresholds for contrails we proceed similarly. In particular, N_{CAS}<0.03 cm^{-3} contains an order of magnitude more observations than the next one. Again, we take a value in the middle (0.4 cm^{-3}) as separation between high N_{CAS} peaks attributable to contrails and moderate values of N_{CAS}<0.4 cm^{-3} that we assign to older contrails/contrail cirrus. Please notice that N and NO are selected independently. Notably, these values are just valid for this flight sequence over the NAR on 26 March 2014 during the ML-CIRRUS campaign.

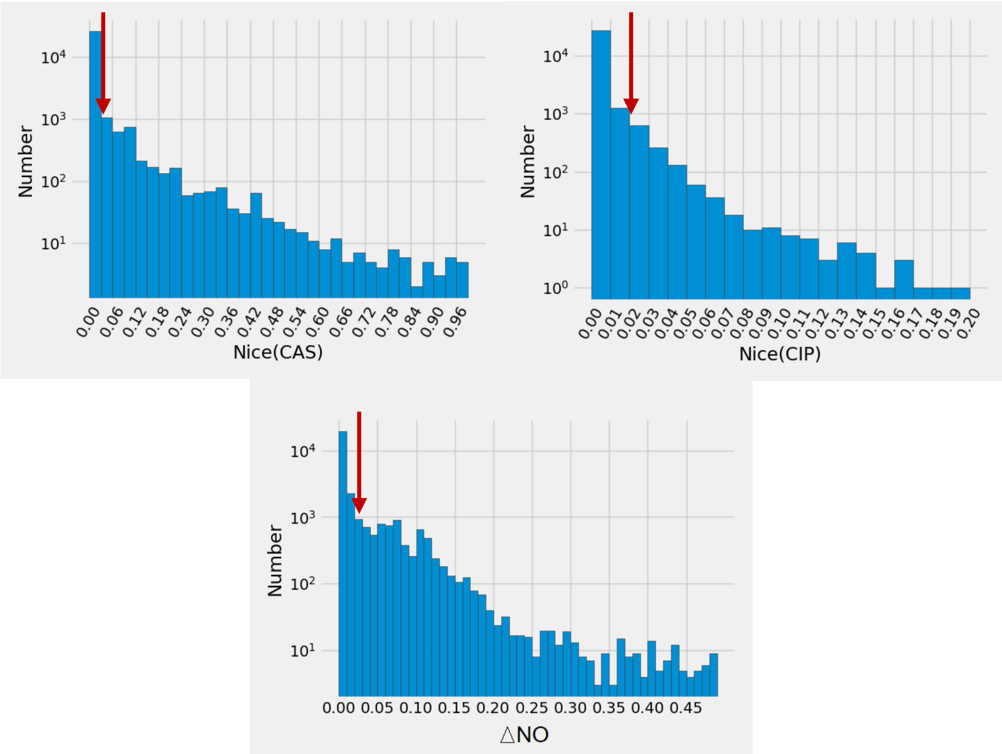

Figure S2: Histograms of in-situ measured Nice from CAS and CIP and ΔNO on 26 March 2014 over NAR.

S4 Evaluation of RRUMS with GERB

To evaluate TOA irradiance from RRUMS during this day, we compare GERB products (RSR_G and OLR_G), comprising 3x3 pixels of MSG/SEVIRI, with RRUMS results along the HALO flight trajectory. Notably, different cirrus classifications have the same TOA value from GERB products and RRUMS results since the temporal/spatial resolution of the in situ data is much higher than that of SEVIRI. We first remove the 7.5% bright bias and 1.3% cold bias of the GERB irradiances in the solar and thermal range (Clerbaux et al., 2009) to build new revised-GERB datasets. We then calculate the 3x3 pixel mean values of RRUMs results. The corresponding RSR_R correlates well with RSR from GERB (RSR_G: correlation coefficient CC=0.72), but RRUMS tends to overestimate GERB (Fig. S3).

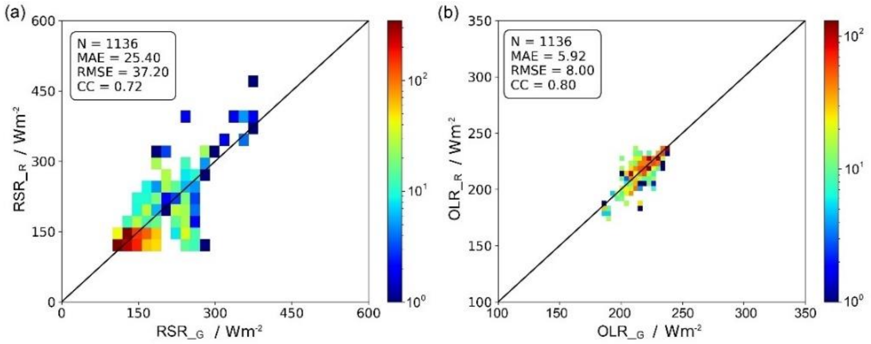

Figure S3: Comparison of TOA (a) RSR and (b) OLR from RRUMS algorithm results (RSR_R, OLR_R) and revised-GERB datasets (RSR_G, OLR_G) (3×3 SEVIRI pixels) along the HALO flight on 26 March 2014. The MAE, RMSE and CC are used as metrics.

In terms of OLR, the agreement is good, with a mean absolute error around 6 W m^{-2} and a correlation coefficient of 0.80 for $OLR_{\_R}$ and $OLR_{\_G}$ (Fig. S3).

Reference

Wandelt, S., and X. Sun: SO6C: Compressed trajectories in air traffic management, J. Intel. Transp. Sys., 16, 844-853, doi: 10.1109/TITS.2014.2345055, 2015.

Clerbaux, N., Russell, J. E., Dewitte, S., Bertrand, C., Caprion, D., De Paepe, B., Gonzalez Sotelino, L., Ipe, A., Bantges, R., and Brindley, H. E.: Comparison of GERB instantaneous radiance and flux products with CERES Edition-2 data, Remote Sensing of Environment, 113, 102-114, https://doi.org/10.1016/j.rse.2008.08.016, 2009.